Preview Control and Its Application to Robot Force Control

예견제어의 로보트 접촉 힘 제어에 대한 응용

Boojoong Yong
(용 부 중)

요 약 : 로보트 매니퓰레이터가 일정한 접촉 힘을 유지하며 공작물의 표면을 따라가게 하는 작업은 많은 자동화 생산공정에서 유용하게 이용될 수 있다. 일반적인 위치제어용 산업용 로보트를 이러한 공정에 사용하기 위해서는 접촉힘이 계측되어 로보트의 제어에 이용되어야만 한다. 이 연구는 accommodation force control 방식으로 산업용 로보트를 제어하여 edge-following에 응용하도록 하며, 접촉 힘의 계측에는 wrist force sensor를 사용한다. 이 시스템의 궤적추적속도와 force regulation 등이 예견제어에 의해 향상될 수 있다. 예견제어에 의해 설계된 전체 제어 시스템은 feedback 제어기와 feedforward 예견제어기로 구성된다. 여기서, 시스템의 안정성은 feedback 제어기에 의해서 결정되며, 예견제어기는 시스템에 미치는 외란을 통제하는 것을 주 기능으로 한다. 일반적인 선형제어 방식을 채택한 경우와 예견제어를 이용한 edge-following을 실험을 통해 비교함으로써, 예견제어의 효용성을 확인한다.

Keywords: preview control, robot force control, contour-following, accommodation control, Kalman filter

I. Introduction

Edge-following is to control a robot manipulator to maintain a constant normal contact force while traversing an unknown irregularly shaped workpiece. Contour-following using a PUMA 560 robot was addressed by Starr [1986]. The experimental results verified the analysis and feasibility of the edge-following task with an accommodation force control [Whitney, 1977] on an industrial robot. Merlet [1987] proposed an approach to determine the surface normal using force measurements with a hybrid position/force controller. Kazanzides *et al.* [1989] developed a dual-drive control, a form of hybrid force/velocity control. They presented a method of determining surface normal and tangential directions from a measured contact force and a robot manipulator velocity. Since commercial robot manipulators often have provision for user-modification of velocity, the accommodation force control is convenient. Only force measurements are necessary, and no modifications need be made to the commercial robot controller. In this paper, a planar edge-following system is modeled according to the accommodation force control in the discrete-time domain.

In an attempt to improve the performance of the contour-following system, this study also investigates the incorporation of a preview control, in an effort to reduce a force error and to increase a tangential tracking speed. Preview control uses the future information about command signals or disturbances as well as instantaneous error signal to the system. The preview control and its applications have been studied by Tomizuka and Whitney [1975], Tomizuka and Rosenthal [1979], Pak and Turner [1986], *etc.* Although much theoretical and simulation work exists using the optimal preview control, experimental realization and performance evaluation of these methods in the robot force control are rarely found. The subject of this paper is investigating the feasibility of the preview control for the robot force control as well as presenting experimental results.

접수일자 : 1996. 2. 17., 수정완료 : 1996. 11. 5.
용부중 : 경북산업대학교 기계공학과

II. Modeling of an edge-following system

Analysis of a force-motion relation involved in a planar edge-following is done using task-related coordinate frames, which are shown in Fig. 1.

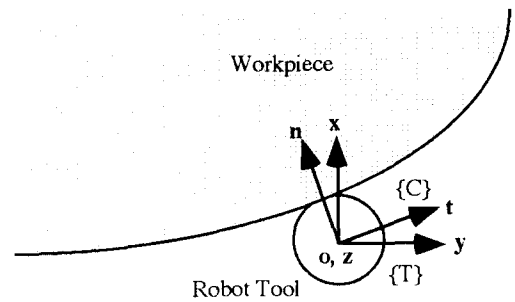

Fig. 1. Tool-workpiece coordinate frames.

Here, {C} denotes the workpiece (contour) constraint frame defined by surface normal (**n**) and tangent (**t**),

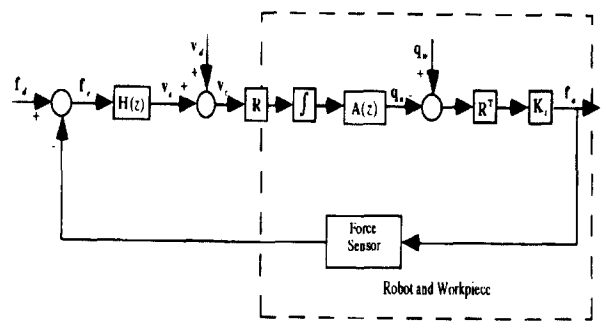

Fig. 2. Block diagram of the contour-following system using accommodation.

$\mathbf{f}_d=\begin{bmatrix} f_d \\ 0 \end{bmatrix}$, $\mathbf{f}_d=\begin{bmatrix} f_a \\ 0 \end{bmatrix}$, $\mathbf{v}_d=\begin{bmatrix} 0 \\ v_d \end{bmatrix}$, $\mathbf{H}(z)=\begin{bmatrix} H(z) & 0 \\ 0 & 0 \end{bmatrix}$,

$\mathbf{A}(z)=\begin{bmatrix} A_x(z) & 0 \\ 0 & A_y(z) \end{bmatrix}$, $\mathbf{K}_t=\begin{bmatrix} K_t & 0 \\ 0 & 0 \end{bmatrix}$.

$\mathbf{f}_d$: desired contact force $\mathbf{f}_e$: force error

$\mathbf{f}_a$: actual contact force

$\mathbf{R}$, $\mathbf{R}^T$: rotation matrices relating tool and constraint frame

$\mathbf{v}_e$: velocity error $\mathbf{v}_d$: desired tangential velocity

$\mathbf{v}_c$: manipulator velocity command

$\mathbf{H}(z)$: force feedback admittance matrix

$\mathbf{K}_t$: total system stiffness matrix

$\mathbf{q}_w$: workpiece position

$\mathbf{q}_a$: actual manipulator tool position

$\mathbf{A}(z)$: robot position dynamic model in Cartesian space

{T} the robot tool frame. In terms of task space partitioning, the normal direction to the contour must be force controlled and the tangential direction of this contour must be position or velocity controlled.

According to the force-motion relation analysis, the complete edge-following system with an accommodation force control appears in Fig. 2. Since this system employs the accommodation, it contains an integrator. Note that $A_x(z)$ and $A_y(z)$, the translational robot arm dynamics, are linear and identical along both x and y axes in the robot tool frame. This is verified by a system identification procedure using experimental data, and is also justifiable partly due to the low velocities and accelerations inherent in the fine motions of the force control, which results in minimal dynamic interaction. The contact force is produced by the interference of the robot and the workpiece through their combined mechanical impedance. Since a robot system with slow motion, *i.e.* low bandwidth, is considered in this work, only the stiffness component of that impedance is modeled. The accommodation force control uses the commercial robot controller which modifies the robot's Cartesian position at a rate of 35Hz. The contact force is measured by a wrist force sensor. The admittance matrix $\mathbf{H}(z)$ determines the nature of the robot's response to changes in contact force.

Contour-following involves both a force control and a velocity control. The desired tangential velocity is fed to the robot positioning system, while the force controller regulates the force error caused by tool/workpiece interactions. Assuming linearity, after designing a force controller, the tangential velocity can be introduced to complete the contour-following system. Since $A(z)=A_x(z)=A_y(z)$, the complex robot arm dynamics are decoupled, and the overall closed-loop transfer function of the edge-following system becomes:

$$\frac{F_a(z)}{F_d(z)}=\frac{\frac{T}{2}\frac{z+1}{z-1}K_tH(z)A(z)}{1+\frac{T}{2}\frac{z+1}{z-1}K_tH(z)A(z)}. \quad (1)$$

T represents a 28ms of sampling period, and $\frac{T}{2}\frac{z+1}{z-1}$ is the Z-transform of an integrator according to Tustin's bilinear rule. The translational PUMA 560 Cartesian closed-loop position dynamics were identified experimentally to be

$$A(z)=0.003343\frac{z+10.3445\pm j7.0804}{(z-0.5890)(z+0.1540\pm j0.3504)}. \quad (2)$$

In general, using a transform-based design method, the outer force-control loop can be designed, at best, as fast as the inner position-control loop [De Schutter and Van Brussel, 1988]. Thus the characteristics of the arm dynamics (rise time, overshoot, settling time, *etc.*) are considered as a design criteria for the linear force controller. If the controller includes the system compliance such that $H(z)=K_t^{-1}D(z)$, it can be designed independent of K_t. Using a root locus method, the linear force controller is designed for the closed-loop system to have dynamic characteristics as close as the robot position dynamics, the conventional linear force controller is

$$D(z)=28.50\frac{z-0.5890}{z+0.5650}. \quad (3)$$

The closed-loop pole locations of the complete system corresponding to this controller are the following:

$$\begin{matrix} z=0.5884\pm j0.1742 \\ z=-0.5256\pm j0.2462 \end{matrix}. \quad (4)$$

(4) shows that the transient mode of the force control loop is very close to the inner position loop. However, irregular or unexpected workpiece position disturbances degrade the performance of the contour-following, thus advanced control technique may be necessary. This will be discussed next.

Ⅲ. Preview control for edge-following of force controlled robot

For edge-following, a geometry of the workpiece contour can be used as a preview information. This *future* geometry may be sensed by a robot-mounted sensor traveling some distance ahead of the robot manipulator. With this future knowledge of the workpiece geometry, a formalism for the preview control is developed in order to improve the performance of the contour-following system [Yong, 1993]. Since practically full measurement of the plant states is not directly accessible, an optimal state estimator is also considered to realize the preview control technique.

3.1 Design of a preview controller

The complete controller consists of two parts: a feedback control and a feedforward preview control. After designing the proper feedback controller, the preview controller will be designed based on the feedback gains. Stability is determined solely by the feedback controller, while the preview controller addresses workpiece position disturbances. The open-loop transfer function of the system, including the designed force controller, is converted to a linear discrete-time state-space equation

such as

$$\begin{aligned} \mathbf{x}(k+1) &= \boldsymbol{\Phi}\mathbf{x}(k) + \boldsymbol{\Gamma}u(k) \\ y(k) &= \mathbf{H}\,\mathbf{x}(k) \end{aligned}, \tag{5}$$

where $\boldsymbol{\Phi}$ is an $n\times n$ system matrix, $\mathbf{x}(k)$ is an n-dimensional state vector, $\boldsymbol{\Gamma}$ is an n-dimensional column vector, $\mathbf{H}$ is an n-dimensional row vector, and $u(k)$ and $y(k)$ are control input and system output, respectively. Considering Fig. 2, as a robot manipulator follows a workpiece surface, the variation of workpiece position causes a force error. Thus the future force errors can be deduced from

$$p(k+i) = K_t\, q_w(k+1)\ ;\ i=1,\cdots,N_p, \tag{6}$$

where $q_w(k+i)$ is a measured quantity of future workpiece position. This future force error will be introduced to the edge-following system as a preview information. Similar to Pak and Turner [1986], the preview servo equation can be modeled as

$$\begin{aligned} \mathbf{p}(k+1) &= \tilde{\boldsymbol{\Phi}}\,\mathbf{p}(k)\ , \\ p(k) &= \tilde{\mathbf{H}}\,\mathbf{p}(k)\ . \end{aligned} \tag{7}$$

$\tilde{\boldsymbol{\Phi}}$ is an $(N_p+1)\times(N_p+1)$ matrix, $\mathbf{p}(k)$ is an (N_p+1)-dimensional preview state vector, $\tilde{\mathbf{H}}$ is an (N_p+1)-dimensional row vector, and

$$\mathbf{p}(k) = [\,p(k)\ \ p(k+1)\ \ p(k+2)\ \cdots\ p(k+N_p)\,]\ ,$$

$$\tilde{\mathbf{H}} = [\,1\ 0\ \cdots\ 0\,]\ ,$$

$$\tilde{\boldsymbol{\Phi}} = \begin{bmatrix} 0 & 1 & 0 & \cdots & \cdot & 0 \\ 0 & 0 & 1 & \cdots & \cdot & 0 \\ \cdot & \cdot & \cdot & \cdots & \cdot & \cdot \\ \cdot & \cdot & \cdot & \cdots & \cdot & \cdot \\ \cdot & \cdot & \cdot & \cdots & 0 & 1 \\ \cdot & \cdot & \cdot & \cdots & -1 & 2 \end{bmatrix}\ .$$

Combining the preview servo model (7) with the plant (5) yields an augmented open-loop system,

$$\begin{aligned} \mathbf{z}(k+1) &= \mathbf{A}\,\mathbf{z}(k) + \mathbf{B}u(k) \\ e(k) &= \mathbf{C}\,\mathbf{z}(k) \end{aligned}, \tag{8}$$

where

$$\mathbf{A} = \begin{bmatrix} \boldsymbol{\Phi} & \mathbf{0} \\ \mathbf{0} & \tilde{\boldsymbol{\Phi}} \end{bmatrix},\ \mathbf{B} = \begin{bmatrix} \boldsymbol{\Gamma} \\ \mathbf{0} \end{bmatrix},\ \mathbf{C} = [\,\mathbf{H}\ \ -\tilde{\mathbf{H}}\,],\ \mathbf{z}(k) = \begin{bmatrix} \mathbf{x}(k) \\ \mathbf{p}(k) \end{bmatrix}.$$

Design of the preview controller requires a performance index, typically defined by

$$J(j) = \frac{1}{2}\sum_{k=j}^{\infty}\{e^{\mathrm{T}}(k)Qe(k) + u^{\mathrm{T}}(k)Ru(k)\}. \tag{9}$$

$e(k)$ represents the force error, R and Q are positive scalar penalty functions, and $(\cdot)^{\mathrm{T}}$ denotes the transpose of $(\cdot)$. Q in the cost function penalizes the force error, while R penalizes large values of the control input. With the given performance index (9) for the augmented system (8), a standard optimal output-regulator will be designed by solving the associated Riccati equation such that

$$\mathbf{S} = \mathbf{A}^{\mathrm{T}}\mathbf{S}\mathbf{A} - \mathbf{A}^{\mathrm{T}}\mathbf{S}\mathbf{B}\{\mathbf{B}^{\mathrm{T}}\mathbf{S}\mathbf{B} + R\}^{-1}\mathbf{B}^{\mathrm{T}}\mathbf{S}\mathbf{A} + \mathbf{C}^{\mathrm{T}}Q\mathbf{C}, \tag{10}$$

where

$$\mathbf{S} = \begin{bmatrix} \mathbf{S}_{11} & \mathbf{S}_{12} \\ \mathbf{S}_{21} & \mathbf{S}_{22} \end{bmatrix},\quad \mathbf{S}_{21} = \mathbf{S}_{12}^{\mathrm{T}}.$$

Note that $\mathbf{S}_{22}$ will not be used to design the controllers, only the dynamic behaviors of $\mathbf{S}_{11}$ and $\mathbf{S}_{12}$ are of importance. $\mathbf{S}_{11}$ and $\mathbf{S}_{12}$ are found to be

$$\mathbf{S}_{11} = \boldsymbol{\Phi}^{\mathrm{T}}\mathbf{S}_{11}\boldsymbol{\Phi} - \boldsymbol{\Phi}^{\mathrm{T}}\mathbf{S}_{11}\boldsymbol{\Gamma}\boldsymbol{\Omega}\boldsymbol{\Gamma}^{\mathrm{T}}\mathbf{S}_{11}\boldsymbol{\Phi} + \mathbf{H}^{\mathrm{T}}\mathbf{Q}\mathbf{H}, \tag{11}$$

$$\mathbf{S}_{12} = \boldsymbol{\Phi}^{\mathrm{T}}\mathbf{S}_{12}\tilde{\boldsymbol{\Phi}} - \boldsymbol{\Phi}^{\mathrm{T}}\mathbf{S}_{11}\boldsymbol{\Gamma}\boldsymbol{\Omega}\boldsymbol{\Gamma}^{\mathrm{T}}\mathbf{S}_{12}\tilde{\boldsymbol{\Phi}} - \mathbf{H}^{\mathrm{T}}\mathbf{Q}\tilde{\mathbf{H}}, \tag{12}$$

where $\boldsymbol{\Omega} = \{\boldsymbol{\Gamma}^{T}\mathbf{S}_{11}\boldsymbol{\Gamma} + R\}^{-1}$. $\mathbf{S}_{11}$ allows a constant optimal feedback gain for the plant if (5) is completely controllable for all time. Then, the corresponding steady-state optimal feedback controller for the plant is

$$\mathbf{K} = \{\boldsymbol{\Gamma}^{\mathrm{T}}\mathbf{S}_{11}\boldsymbol{\Gamma} + \mathrm{R}\}^{-1}\boldsymbol{\Gamma}^{\mathrm{T}}\mathbf{S}_{11}\boldsymbol{\Phi}. \tag{13}$$

Since (12) shows $\mathbf{S}_{12}$ depends on $\mathbf{S}_{11}$, the constant feedforward preview gain (preview controller) can be determined according to $\mathbf{S}_{11}$ [Yong and Starr, 1993]; it yields

$$\mathbf{K}_{ff} = \{\boldsymbol{\Gamma}^{\mathrm{T}}\mathbf{S}_{11}\boldsymbol{\Gamma} + R\}^{-1}\boldsymbol{\Gamma}^{\mathrm{T}}\mathbf{S}_{12}\tilde{\boldsymbol{\Phi}} = [\,0\ \ \mathbf{K}_{pr}\,]. \tag{14}$$

Finally the control input $u(k)$ for the plant (5) becomes

$$\begin{aligned} u(k) &= -\mathbf{K}_{sys}\mathbf{z}(k) \\ &= -[\,\mathbf{K}\ \ \mathbf{K}_{ff}]\mathbf{z}(k) \\ &= -\mathbf{K}\,\mathbf{x}(k) - \mathbf{K}_{pr}\,\bar{\mathbf{p}}(k) \end{aligned}\ , \tag{15}$$

where $\bar{\mathbf{p}}(k) = [\,p(k+1)\ \ p(k+2)\ \cdots\ p(k+N_p)\,]^{\mathrm{T}}$. $\mathbf{K}$ is the time-invariant optimal feedback controller (n-dimensional gain vector) and $\mathbf{K}_{pr}$ is the constant feedforward preview controller (N_p-dimensional gain vector). If the preview length is zero ($N_p=0$), *i.e.*, future force errors are not used for the control system, the control structure reduces to a conventional optimal control.

3.2 Edge-following using preview controller and optimal state estimator

Since the full system state $\mathbf{x}(k)$ is not directly accessible, a state estimator is required in the feedback loop. Some disturbances and modeling inaccuracies between the actual plant and the estimator model can result in unbounded estimation errors, *i.e.*, the estimator may not be stable. For this reason, an optimal state estimator, which handles noise contaminated systems effectively, is chosen for the estimator design. Optimal estimation methods combine the information from the noisy measurements with the information implicit in the estimator model equation [Lewis, 1986]. Considering noise effects on the system, let an estimator model be described by a linear time-invariant discrete-time equation,

$$\begin{aligned} \mathbf{x}(k+1) &= \boldsymbol{\Phi}\,\mathbf{x}(k) + \boldsymbol{\Gamma}u(k) + \boldsymbol{\Gamma}_w w(k), \\ y(k) &= \mathbf{H}\,\mathbf{x}(k) + v(k), \end{aligned} \tag{16}$$

where the process noise $w(k)$ and the measurement noise $v(k)$ are random sequences with zero mean and

white noise. If the output error signal $e(k)$ is fed back, the estimated state vector $\hat{\mathbf{x}}(k)$ can be obtained such as

$$\hat{\mathbf{x}}(k) = \bar{\mathbf{x}}(k) + \mathbf{L}\{e(k) - \mathbf{H}\,\bar{\mathbf{x}}(k)\}, \tag{17}$$

where $\mathbf{L}$ is the constant Kalman gain, and $\bar{\mathbf{x}}(k)$ is a time updated state from

$$\bar{\mathbf{x}}(k+1) = \boldsymbol{\Phi}\,\hat{\mathbf{x}}(k) + \boldsymbol{\Gamma} u(k). \tag{18}$$

Fig. 3 shows the edge-following system enhanced by the preview controller along with the Kalman filter.

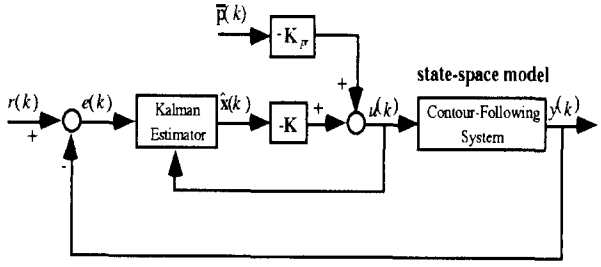

Fig. 3. Edge-following system with optimal preview control and Kalman filter.

In Fig. 3, the external reference input $r(k)$ is the desired normal contact force, $y(k)$ the actual contact force. Note that the feedback portion is a series of the optimal state estimator and the optimal controller, while the feed-forward portion is a weighted sum of previewed values of force errors.

3.3 Implementation of preview controller on the contour-following system

To implement the preview controller on the standard edge-following system, the plant model (5) is described by a 4th-order observer canonical form, such that

$$\boldsymbol{\Phi} = \begin{bmatrix} 0.12699 & 1 & 0 & 0 \\ 0.55246 & 0 & 1 & 0 \\ 0.23776 & 0 & 0 & 1 \\ 0.08278 & 0 & 0 & 0 \end{bmatrix}, \tag{19}$$

$$\boldsymbol{\Gamma} = \begin{bmatrix} 0.00133 \\ 0.02893 \\ 0.23719 \\ 0.20959 \end{bmatrix}, \quad \mathbf{H} = [1\ 0\ 0\ 0].$$

The feedback controller is designed by adjusting a weighting factor ratio ($\rho_c = \frac{Q}{R}$) in the performance index (9) until a satisfactory transient response is obtained, thus the design requires a certain amount of iteration. The feedback gain and the 5-step preview gain are found to be:*)

$$\mathbf{K} = [1.3820\ \ 1.5905\ \ 1.0099\ \ 2.3094], \tag{20}$$
$$\mathbf{K}_{pr} = [-0.0144\ \ -0.3030\ \ -2.3652\ \ -0.5137\ \ -0.0892].$$

The steady-state Kalman gain is also computed for selected value of noise covariances. Since actual process noise covariance is not available, final gain selection is done experimentally so that the filter removes the undesired oscillation without introducing too much lag and slowing the response. The determined Kalman gain is:

$$\mathbf{L} = [0.3599\ \ 0.3040\ \ 0.0801\ \ 0.0193]^{T}. \tag{21}$$

*) Among several preview steps tested for experiments, 5-step preview yields most appropriate result. Theoretically more preview will result in better performance. However, in reality, a preview beyond a critical limit may degrade the performance, possibly due to inaccurate preview information and/or actuator limits.

Ⅳ. Experimental Results

Experiments were performed using a PUMA 560 manipulator with unmodified Unimation controller and a 6-axis wrist force sensor. The PUMA 560 robot was controlled by an external VME computer which coordinates the robot manipulator and the force sensor. Total system contact stiffness K_t was measured to be 13.85 N/mm. A potentiometer was used for a preview sensor.

Two planar edge-following systems, the standard system using a conventional linear controller and the system enhanced by an optimal preview controller, were tested on three separate tasks at a tangential speed of 20mm/sec.: (1) following a straight edge, (2) responding to a 30° step change in the contour, and (3) following a curved contour of 40mm radius of curvature. Fig. 4 shows the workpiece contours for experimental evaluations.

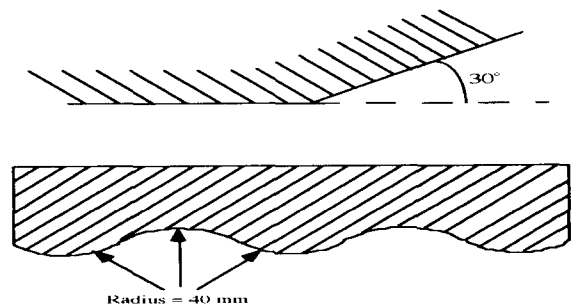

Fig. 4. Workpiece contours with a 30° step change and 40mm radius of curvature.

Performance was characterized in two ways: the comparison of rms (root-mean-square) force error, and the amount of increase in tangential tracking speed which can be tolerated while maintaining a contact force within a certain range. The second measure is an indication of the robustness of the system.

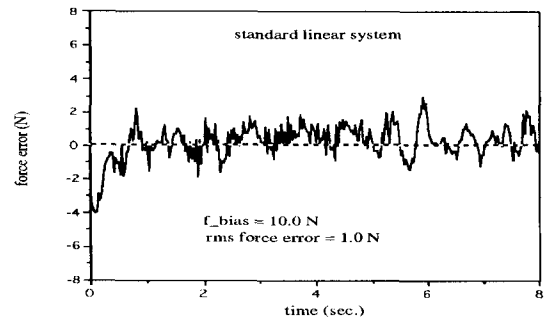

Fig. 5. Following a straight edge with conventional linear controller.

4.1 Following a Straight Edge

Following a straight edge (Figures 5~6), force error profiles for both systems are almost indistinguishable. It is true that we do not expect workpiece disturbances in the straight edge-following. Meanwhile maximum tangential tracking speed was improved about 22% (from 58mm/sec. to 71mm/sec.) using the preview control, staying within the given bias force range of 9.5N~13.0N. Noisy signals (oscillations) while following an edge reflects mechanical vibrations on the robot manipulator and unmodeled higher frequency dynamics.

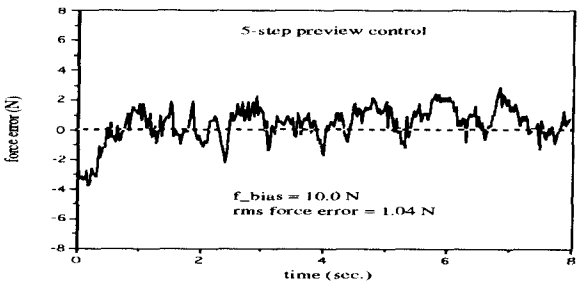

Fig. 6. Following a straight edge with preview controller.

4.2 Encountering a step change in contour

Figures 7~8 show force errors encountering a step change in the contour angle. The conventional linear control system is more sensitive to the immediate workpiece position disturbance. On the other hand, the peak force error is sufficiently suppressed by the preview control. Since our interest in this test is the rejection of the step disturbance, the rms force error is not calculated. The preview controller achieves higher tracking speed (30mm/sec.) compared to the conventional linear controller (23mm/sec.).

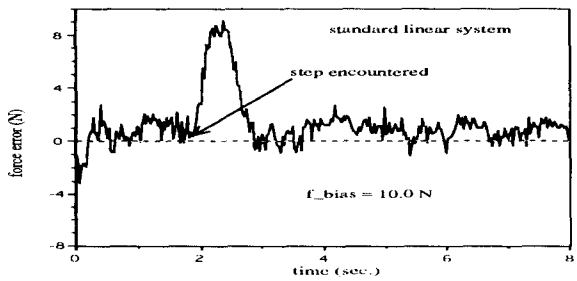

Fig. 7. Response to a step in 30° with conventional linear controller.

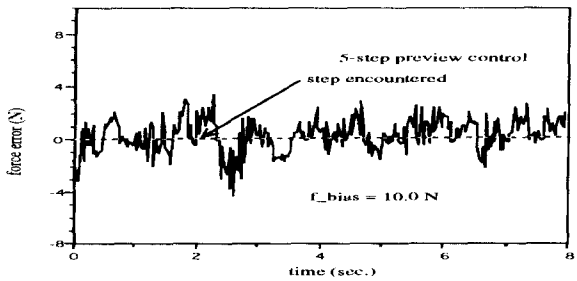

Fig. 8. Response to a step in 30° with preview controller.

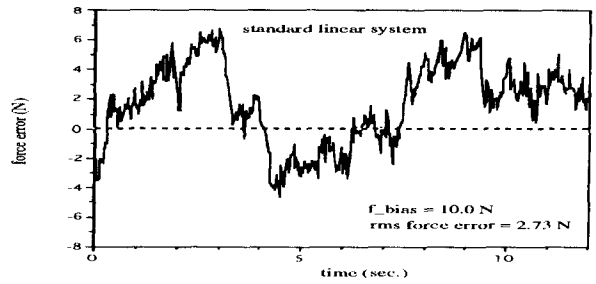

Fig. 9. Following a curved contour with conventional linear controller.

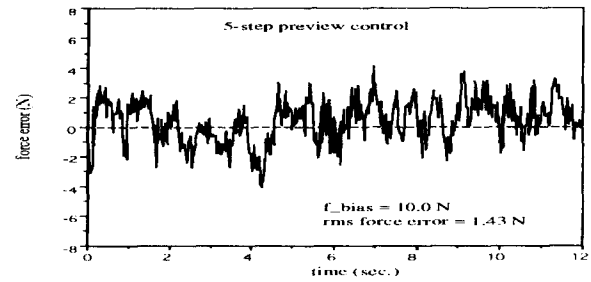

Fig. 10. Following a curved contour with preview controller.

4.3 Following a curved contour

The workpiece position disturbance is approximately sinusoidal with the curved contour shown in Fig. 4. The experimental results presented in Figures 9~10 show that the peview control is very effective in reducing the force error due to this type of sinusoidal disturbance. The preview controller yields much narrower force error envelope compared to the nonpreview control system. Maximum tangential tracking speed by the preview control was increased from 23mm/sec. to 30 mm/sec.

V. Conclusion

A planar contour-following is designed using an accommodation force control. A preview controller with a Kalman filter is applied to the standard edge-following system, which uses a conventional linear force controller, in order to improve the performance of the contour -following. For experimental verification the designed systems - the standard system and the system enhanced by the preview control - are tested using a PUMA 560 robot.

This study shows that the preview control method is very useful for the robot force control. The preview control provides a portability on the pre-existing linear controller, *i.e.*, it can be used as an enhancement. Experimental results manifest that the preview control reduces the contact force error as well as increases the tangential tracking speed while performing the edge-following task. It is found that short preview steps ($N_p=5$) are enough to accomplish the performance improvement obtained by the preview control. It also can be seen that the effect of preview is most noticeable at sharp corners or on a continuously curving contour.

References

[1] De Schutter, J., Van Brussel, H., "Compliant motion: II. A control approach based on external control loops," *International Journal of Robotics Research*, vol. 7, no. 4, Aug., 1988.

[2] P. Kazanzides, N. S. Bradley and W. A. Wolovich, "Dual-drive force/velocity control : Implementation and experimental results," *Proc. IEEE International Conf. on Robotics and Automation*, 1989.

[3] F. L. Lewis, *Optimal Estimation*, John Wiley & Sons, Inc., 1986.

[4] J. -P. Merlet, "C-surface applied to the design of an hybrid force-position robot controller," *Proc. IEEE Int. Conf. on Robotics and Automation*, 1987.

[5] H. A. Pak and P. J. Turner "Optimal tracking controller design for invariant dynamics direct drive arms," *ASME Journal of Dynamic Systems, Measurement, and Control*, vol. 108, June, 1986.

[6] G. P. Starr, "Edge-following with a PUMA 560 Manipulator Using VAL-II," *Proc. IEEE Int. Conf. on Robotics and Automation*, 1986.

[7] M. Tomizuka and D. E. Whitney, "Optimal discrete finite preview problems (why and how is future information important ?)," *ASME Journal of Dynamic Systems, Measurement, and Control*, Dec., 1975.

[8] M. Tomizuka and D. E. Rosenthal, "On the optimal digital state vector feedback controller with integral and preview actions," *ASME Journal of Dynamic Systems, Measurement, and Control*, vol. 101, June, 1979.

[9] D. E. Whitney, "Force feedback control of manipulator fine motions," *ASME Journal of Dynamic Systems, Measurement, and Control*, June, 1977.

[10] B. Yong, "Preview control for robot force control," *Ph. D. Dissertation*, Univ. of New Mexico, May, 1993.

[11] B. Yong and G. P. Starr, "Application of preview control to contour-following using a force-controlled industrial robot," *Proc. ASME 14th Biennial Conference on Mechanical Vibration and Noise*, Albuquerque, NM, Sep., 1993.

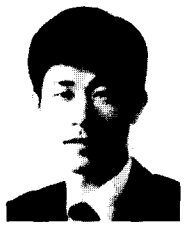

용 부 중

1985년 인하대학교 기계공학과 학사. 1987년 Univ. of New Mexico 기계공학과 석사. 1993년 Univ. of New Mexico 기계공학과 박사. 1994년~1995년 한국항공우주연구소 선임연구원. 1995년~현재 경북산업대학교 전임강사. 관심분야는 Robotics and Control, Preview Control System.